Originally published in Moecular Oncology. 2015 Sep 25. pii: S1574-7891(15)00165-9. doi: 10.1016/j.molonc.2015.09.006. The original version of this paper is available at http://www.moloncol.org/article/S1574-7891(15)00165-9/abstract

Altered purinergic receptor-Ca^{2+}signaling associated with hypoxia-induced epithelial-mesenchymal transition in breast cancer cells

Iman Azimi[a, f], Hannah Beilby[a], Felicity M. Davis[a,1], Daneth L. Marciala[a], Paraic A. Kenny[b], Erik W. Thompson[c, d, e], Sarah J. Roberts-Thomson[a], Gregory R. Monteith[a,f,*]

[a]School of Pharmacy, The University of Queensland, Brisbane, Queensland, Australia

[b]Kabara Cancer Research Institute, Gundersen Medical Foundation, La Crosse, Wisconsin, United States of America

[c]Institute of Health and Biomedical Innovation and School of Biomedical Sciences, Queensland University of Technology, Kelvin Grove, Queensland, Australia

[d]University of Melbourne Department of Surgery, St Vincent's Hospital, Fitzroy, Victoria, Australia

[e]St Vincent's Institute, Fitzroy, Victoria, Australia

[f]Mater Research Institute, The University of Queensland, Translational Research Institute, Brisbane, Queensland, Australia

***Corresponding Author**: Gregory R. Monteith, School of Pharmacy, The University of Queensland, Brisbane, Queensland, Australia. Phone: +61 733461855; Fax: +61 733461999; Email: gregm@uq.edu.au

[1]Present Address: Department of Pathology, The University of Cambridge, Cambridge, United Kingdom

Abstract

Hypoxia is a feature of the microenvironment of many cancers and can trigger epithelial-mesenchymal transition (EMT), a process by which cells acquire a more invasive phenotype with enriched survival. A remodelingof adenosine 5′-triphosphate (ATP)-induced Ca^{2+}signaling via purinergic receptors is associated with epidermal growth factor (EGF)-induced EMT in MDA-MB-468 breast cancer cells. Here, we assessed ATP-mediated Ca^{2+} signaling in a model of hypoxia-induced EMT in MDA-MB-468 cells. Like EGF, hypoxia treatment (1% O_2) was also associated with a significant reduction in the sensitivity of MDA-MB-468 cells to ATP (EC_{50} of 0.5 μM for normoxic cells versus EC_{50} of 5.8 μM for hypoxic cells). Assessment of mRNA levels of a panel of P2X and P2Y purinergic receptors following hypoxia revealed a change in levels of a suite of purinergic receptors. P2X4, P2X5, P2X7, P2Y1 and P2Y11 mRNAs decreased with hypoxia, whereas P2Y6 mRNA increased. Up-regulation of P2Y6 was a common feature of both growth factor- and hypoxia-induced models of EMT. P2Y6 levels were also significantly increased in basal-like breast tumors compared to other subtypes and breast cancer patients with higher P2Y6 levels showed reduced overall survival rates. P2Y6 siRNA-mediated silencing and the P2Y6 pharmacological inhibitor MRS2578 reduced hypoxia-induced vimentin protein expression in MDA-MB-468 cells. P2Y6 inhibition also reduced the migration of mesenchymal-like MDA-MB-231 breast cancer cells.The up-regulation of P2Y6 appears to be a common feature of the mesenchymal phenotype of breast cancer cells and inhibition of this receptor may represent a novel therapeutic target in breast cancer metastasis.

Keywords

Breast cancer, hypoxia, calcium, epithelial-mesenchymal transition, purinergic receptors

Abbreviations:

ATP, adenosine 5′-triphosphate; $[Ca^{2+}]_{CYT}$, cytosolic free Ca^{2+}; EMT, epithelial-mesenchymal transition; EGF, epidermal growth factor; FBS, fetal bovine serum; HMEC, human mammary epithelial cells; FLIPR, Fluorometric Imaging Plate Reader; IP3, 1,4,5 inositol trisphosphate; ROI, region of interest.

1. Introduction

Epithelial-mesenchymal transition (EMT) in cancer cells is a complex series of molecular and cellular events by which epithelial cells reduce their epithelial-specific characteristics and acquire a mesenchymal phenotype (Polyak and Weinberg, 2009). In this process, cells lose their polarity and cell-cell adhesion, and convert to fibroblastoid cells with invasive and migratory abilities (Grunert et al., 2003; Polyak and Weinberg, 2009). Down-regulation of epithelial markers such as E-cadherin and up-regulation of mesenchymal markers such as N-cadherin and vimentin are common features of EMT (Jiang et al., 2011; Thiery, 2002).

EMT can be triggered by several stimuli including growth factor signaling and stromal cell-epithelial cell interactions in the tumor microenvironment (Polyak and Weinberg, 2009; Thiery and Sleeman, 2006). Hypoxia is a feature of the tumor microenvironment where there is a reduction in normal oxygen levels. Hypoxic microenvironments may promote adaptive survival programs, which are often associated with resistance to apoptosis, angiogenesis and migration (Ruan et al., 2009). Recent studies show that hypoxia induces EMT in a variety of cancer cell types (Cannito et al., 2008; Cooke et al., 2012; Misra et al., 2012; Sahlgren et al., 2008; Salnikov et al., 2012; Shaikh et al., 2012; Zhang et al., 2013), including the MDA-MB-468 cell line used in our study (Cursons et al., 2015; Jo et al., 2009; Lundgren et al., 2009).

Calcium is a highly versatile intracellular messenger, which can play a crucial role in many of the cancer hallmarks including proliferation (Akl and Bultynck, 2013; Roderick and Cook, 2008), angiogenesis (Chen et al., 2011; Munaron and Fiorio, 2009) and metastasis (Prevarskaya et al., 2011). We have recently characterized a role for Ca^{2+}signaling in the *induction* of EMT (Davis et al., 2013) and reported changes in Ca^{2+} influx and adenosine 5′-triphosphate (ATP)-mediated Ca^{2+}signaling as a *consequence* of EMT induced by epidermal growth factor (EGF) (Davis et al., 2012). The tumor microenvironment is rich in ATP, and therefore increases in intracellular free Ca^{2+} levels via activation of plasmalemmal purinergic receptors are likely (Maehara et al., 1987; Pellegatti et al., 2008). Increases in intracellular Ca^{2+} can be achieved directly through the influx of Ca^{2+} via ligand-gated ionotropic P2X receptors or indirectly through activation of G-proteins and the generation of 1,4,5 inositol trisphosphate (IP_3) by metabotropic P2Y receptors (Burnstock and Di, 2013).

EGF-induced EMT in MDA-MB-468 breast cancer cells is associated with alterations in ATP-mediated Ca^{2+} increases, with a significant increase in the EC_{50} of ATP as a consequence of EMT induction (0.175 μM to 1.731 μM) (Davis et al., 2011). Assessment of the expression of P2X and P2Y

receptors after EGF-induced EMT revealed a remodeling of purinergic receptor isoform mRNA, with increases in P2X5 and P2Y6 levels and a down-regulation of P2Y13 (Davis et al., 2011). Here, we sought to investigate changes in ATP-mediated Ca^{2+}signaling and purinergic receptor expression in a hypoxia-induced model of EMT to determine whether alterations in ATP-mediated Ca^{2+}signaling are a common feature of EMT in MDA-MB-468 breast cancer cells, irrespective of the inducing stimuli.

2. Materials and methods

2.1. Cell culture and hypoxia induction

MDA-MB-468 and MDA-MB-231 human breast cancer cells were maintained in Dulbecco's Modified Eagle's Medium (DMEM; D6546 Sigma Aldrich, St Louis, MO, USA) supplemented with 100 U/mL Penicillin G and 100 µg/mL streptomycin sulphate (Sigma Aldrich), 10% fetal bovine serum (FBS) and 4 mM L-glutamine at 37°C with 5% CO2. To induce EMT, MDA-MB-468 cells were serum starved (0.5% FBS) for 24 h and maintained in a humidified incubator (37°C, 5% CO_2) with 21% O_2 (normoxia) or 1% O_2 in a Sanyo MCO-18M multi-gas incubator (hypoxia). Cells were maintained in hypoxia for 24 h (gene expression) or 48 h (protein and calcium assays). These time points were chosen because changes in mRNA levels are expected to precede changes in protein levels and functional responses. MDA-MB-231 cell lines were obtained directly from American Type Culture Collection. MDA-MB-468 cells were obtained as previously described (Davis et al., 2011). MDA-MB-231 and MDA-MB-468 cells were cultured for less than 10 passages (5–6 weeks) in this study. Cell lines were regularly screened every 6 months for mycoplasma contamination (MycoAlert; Lonza Basel, Switzerland) and also monitored for morphological characteristics.STR profiling was performed by Queensland Institute of Medical Research using the StemElite ID Profiling Kit (Promega Madison, WI, USA).

2.2. Immunoblotting

Samples were resolved on NuPAGENovex 4–12% BisTris gels (Invitrogen, Carlsbad, CA, USA) with MOPS running buffer under reducing conditions and transferred to polyvinylidene difluoride membranes as described previously (Davis et al., 2011). Proteins were detected using 1:750 dilution of mouse anti-vimentin V9 monoclonal antibody (V6389, Sigma Aldrich)and 1:100 dilution of hECD1 mouse anti-E-cadherin (a kind gift from Professor Alpha Yap, The University of Queensland, Australia). A 1:10,000 dilution of goat anti-mouse horseradish peroxidase-conjugated (170-6516, Bio-

Rad, Hercules, CA, USA) was used as the secondary antibody. For detection of P2Y6 protein, 1:20,000 dilution of rabbit-anti P2Y6 monoclonal antibody (LS-C105670, LifeSpanBioSciences, Inc, Seattle, WA, USA) and a 1:10,000 dilution of goat anti-rabbit horseradish peroxidase-conjugated secondary (170–6515, Bio-Rad) were used.Antibodies were prepared in phosphate buffered saline (PBS) solution containing 5% (w/v) skim milk powder and 0.1% Tween-20. Chemiluminescence blots were analyzed using a VersaDoc Imaging System (BioRad) and the density of each band was quantified by Quantity One (version 4.6.7, Bio-Rad) and normalized to its relative β-actin band.

2.3. Measurement of intracellular free Ca^{2+}

Increases in cytosolic free Ca^{2+} ($[Ca^{2+}]_{CYT}$) after purinergic receptor activation was assessed in normoxic and hypoxic MDA-MB-468 cells with a Fluorometric Imaging Plate Reader ($FLIPR^{TETRA}$, Molecular Devices, Sunnyvale, CA, USA) using the BD PBX no-wash Ca^{2+} Assay Kit (BD Biosciences, Franklin Lakes, NJ, USA) as previously described (Grice et al., 2010). Cells were seeded at 3 x 10^4 cells per well in 96-well black plates (Corning Costar, Cambridge, MA, USA) and 24 h post seeding, cells were serum-deprived (0.5% FBS) for 24 h and were either left in normoxia or placed under hypoxic conditions for 24 h. Cells were loaded for 60 min at 37°C with 2 μM PBX Calcium Indicator dye in a solution containing 5% (v/v) PBX Signal Enhancer and 500 μM probenecid in physiological salt solution (PSS; 5.9 mMKCl, 1.4 mM MgCl2, 10 mM HEPES, 1.2 mM NaH2PO4, 5 mM NaHCO3, 140 mMNaCl, 11.5 mM glucose, 1.8 mM $CaCl_2$). Cells were equilibrated to room temperature for 15 min and dye loading solution was then replaced with a solution containing 5% (v/v) PBX Signal Enhancer and 500 μM probenecid in PSS. Fluo-4 fluorescence intensity was assessed using 470-495 nm excitation and 515-575 nm emission filters. ScreenWorks Software (v2.0.0.27, Molecular Devices) was used for data analysis. Response over baseline was assessed as a relative measure of $[Ca^{2+}]_{CYT}$.

2.4. siRNA silencing and P2Y6 pharmacological inhibition

Dharmacon ON-TARGETplusSMARTpool siRNA (Thermo Scientific, Waltham, MA, USA) was used for the knockdown of P2Y6 (L-004579-00-0005) and HIF1α (L-004018-00-0005) genes (100 nM). DharmaFECT4 Transfection Reagent (0.1 μl per well) was used for siRNA transfection. MDA-MB-468 cells were seeded at 6 x 10^4 (48 h hypoxia) or 1 x 10^5 (24 h hypoxia) cells per well in a 96-well plate.

Cells were transfected with siRNA 24 h after seeding. Cells were serum starved (0.5% FBS) 48 h after siRNA transfection for 24 h. Cells were then exposed to hypoxic conditions (1% O_2) for 24 h or 48 h.

For pharmacological inhibition studies, cells were seeded at 2 x 10^5 cells per well (96 well plate) and then the P2Y6 inhibitor MRS2578 added 24 h after plating in serum reduced-media (0.5 % FBS) for 24 h. Cells were then placed under hypoxic conditions (1% O_2) for 24 h.

2.5. Real time RT-PCR

These studies focused on purinergic receptor mRNA levels after hypoxia, as has been done for EGF in this model (Davis et al., 2011), due to the lack of sufficiently selective antibodies for all purinergic receptor isoforms (Coakley et al., 2008; Griffiths and Lucocq, 2014; Yu and Hill, 2013).Total RNA from MDA-MB-468 cells was isolated and purified using RNeasy Plus Mini Kit (Qiagen, Hilden, Germany). The purified RNA was reverse transcribed using Omniscript RT Kit (Qiagen) and the target cDNA was amplified using TaqMan® Fast Universal PCR Master Mix (Applied Biosystems, Carlsbad, CA, USA) and TaqMan® gene expression assays. A StepOnePlus™ instrument (Applied Biosystems) was used to cycle and quantitate targets. The comparative C_T ($\Delta\Delta C_T$) method was used to determine the relative target quantity by normalizing to 18S ribosomal RNA. The TaqMan® gene expression assay used for P2Y6 receptor was Hs00602548_m1 and the assays IDs for the panel of P2X and P2Y receptors used in the Custom TaqMan Array are included in Supplementary Table S1.

Gene expression assays used to assess EMT markers included: vimentin (Hs00185584_m1), Twist (Hs00361186_m1), Snail (Hs00195591_m1), N-cadherin (Hs00983062_m1), CD24 (Hs02379687_s1), CD44 (Hs01075861_m1), and Zeb1 (Hs00232783_m1).

2.6. Cell migration assay

The effect of the P2Y6 inhibitor on cell migration of MDA-MB-231 cells was assessed using the Oris™ Cell Migration Assembly Kit (CMAUFL4, Platypus Technologies). The Oris™ Cell Seeding stoppers were placed in the centre of each well to create a 2 mm diameter detection zone, and cells were seeded at 1.5 x 10^4 cells per well in Oris™-compatible 96-well black plates. The stoppers were removed 48 h post seeding, and the cells were then washed once with media. Fresh media containing MRS2578 or DMSO (matched solvent control) was then added to cells. The microplate was then placed in an incubator for 24 h to allow cells to migrate into the detection zone. Cells were loaded for 60 min at 37°C with 0.5 μMcalcein AM (Life Technologies) in a solution containing 0.5 mMprobenecid

and 5% (v/v) PBX signal enhancer (BD Biosciences) in growth media. Cell migration was assessed using an ImageXpress Micro (Molecular Devices) automated epifluorescent microscope with 472/30 excitation and 520/35 emission filters. Cell migration was quantified using an algorithm that positioned a 2 mm (equivalent diameter to stopper) region-of-interest (ROI) at the center of the detection zone and calculated the area of cells inside the ROI. Migrated area measurements for the control and treatment replicates where normalized to the average of control (DMSO) measurements.

2.7. Gene expression microarray

Gene expression profiles of human breast tumors with matched exome sequencing data (n=466) were obtained from the TCGA study (Koboldt et al., 2012). These included 81 basal-like, 53 HER2, 210 Luminal A, 114 Luminal B, and 8 Normal-like tumors. Samples assigned to the Normal-like subtype were excluded, as they are believed to be substantially contaminated by normal tissue(Giricz et al., 2013). P2Y6 expression was evaluated in all samples and the median levels of the expression of this gene were compared between tumors of each subtype using the Kruskal-Wallis test with Dunn's post-test.

Gene expression profile of P2Y6 was also assessed in the publically available E-MTAB-181 microarray dataset of 49 breast cancer cell lines and 5 nonmalignant immortalized human mammary epithelial cells (HMEC) (Heiser et al., 2012). These cell lines represent three subgroups of Luminal (predominantly luminal; equivalent to Luminal and HER2 breast cancer subtypes), Basal A (mixed basal/luminal; equivalent to Basal breast cancer subtype), and Basal B (equivalent to Mesenchymal subgroup with enhanced invasive features; equivalent to Claudin Low breast cancer subtype) (Neve et al., 2006; Prat et al., 2010).

2.8. Survival analysis

To assess the association between P2Y6 expression level and patient overall survival, a Kaplan-Meier plot was generated using the publically available Kaplan-Meier Plotter at http://www.kmplot.com(Gyorffy et al., 2010) using the probe 208373_s_at. Overall survival was assessed for 1115 patients using a median cutpoint derived from all of the breast tumors in the KMPlot dataset. Statistical significance of the survival curve was calculated using the log-rank analysis.

2.9. Statistical analysis

Statistical tests used have been described in each figure legend. Data analysis was performed using GraphPad Prism version 5.04 for Windows (GraphPad Software, Inc., La Jolla, CA, USA).

3. Results

3.1. Hypoxia alters the nature of the cytosolic calcium response to ATP

The induction of EMT by hypoxia was confirmed by quantifying mRNA and protein levels of key EMT markers, and by assessment of morphological changes of the cells. The mRNA levels of vimentin, N-cadherin, Twist, Snail, Zeb1, and the CD44/CD24 mRNA ratio (a marker of stem cell-like phenotype associated with EMT (Balko et al., 2013)), were all significantly increased in hypoxic cells (1% O_2, 24 h) compared to normoxic cells (Fig. 1A). Incubation of cells in hypoxia for 48 h significantly elevated protein levels of vimentin (Fig. 1B) and attenuated protein expression of the epithelial marker, E-cadherin (Fig. 1C). After 48 h of hypoxia, MDA-MB-468 cells acquired a spindle-shaped morphology characteristic of a more mesenchymal phenotype (Fig. 1D).

Incubation of cells in hypoxic conditions for 48 h altered intracellular Ca^{2+} responses to 1 mM ATP (Fig. 2A), with a reduction in the maximum $[Ca^{2+}]_{CYT}$ response and a faster recovery of $[Ca^{2+}]_{CYT}$ to resting levels. MDA-MB-468 cells were also less sensitive to ATP after hypoxia, with a rightward shift in the concentration response curve (EC_{50} of 0.5 μM for normoxic cells versus EC_{50} of 5.8 μM for hypoxic cells) (Fig. 2B). To quantify differences in the recovery phase of the cytosolic calcium transient we calculated percent recovery at the end of the assay. These results confirm that MDA-MB-468 cells maintained under hypoxia have a faster return to baseline calcium levels compared to cells maintained in normoxia (Fig. 2C). The observed changes in $[Ca^{2+}]_{CYT}$ with hypoxia in response to ATP could be due in part to alterations in the expression of purinergic receptors with hypoxia.

3.2. Hypoxia modifies the transcriptional profile of purinergic receptors in MDA-MB-468 cells

We assessed mRNA levels of a panel of seven ionotropic P2X and eight metabotropic P2Y subtypes in normoxic and hypoxic MDA-MB-468 cells (Fig. 3A). For both treatments, mRNA levels for P2X1, P2X2, P2X3, P2X6, P2Y12, P2Y13 and P2Y14 were not detected with real time RT-PCR. P2Y2 and

P2Y4 mRNA levels were not altered by hypoxia.Hypoxia was associated with a decrease in P2X4, P2X5, P2X7, P2Y1 and P2Y11 mRNAs levels (Fig. 3A), whereas levels of P2Y6 mRNA increased with hypoxia (~3-fold, Fig. 3A and B).We also confirmed the up-regulation of P2Y6 expression by hypoxia at the protein levels by immunoblotting (Fig. 3C). Our previous studies on the expression of P2 receptors in EGF-induced EMT showed a 2.1-fold increase in P2Y6 mRNA expression in EGF-treated samples (Davis et al., 2011). P2Y6 was the only P2 receptor that was up-regulated in both EGF- and hypoxia-induced EMT in MDA-MB-468 cells (Fig. 3D). Up-regulation of P2Y6 mRNA was partially dependant on HIF1α as siRNA silencing of HIF1α (Fig. 3E left) reduced hypoxia-induced P2Y6 mRNA up-regulation (Fig. 3E right).

To determine if P2Y6 may be involved in some aspects of EMT induction the effects of P2Y6 siRNA-mediated silencing and the P2Y6 selective inhibitor MRS2578 on hypoxia-induced EMT were assessed.

3.3. P2Y6 silencing and pharmacological inhibition attenuates hypoxia-induced vimentin expression

siRNA-mediated silencing of P2Y6 (Fig. 4A), significantly reduced protein expression of the EMT marker vimentin at 48 h (Fig. 4B). However, silencing of P2Y6 had no significant effect on hypoxia-mediated changes in the mRNA levels of vimentin, N-cadherin, Snail and Twist, or the CD44/CD24 ratio (Fig. 4C). The effects of the P2Y6 pharmacological inhibitor MRS2578 (Chadet et al., 2014; Mamedova et al., 2004) on hypoxia-mediated EMT induction was also assessed. Pre-incubation of MDA-MB-468 cells with MRS2578 significantly attenuated hypoxia-induced vimentin protein expression at 3 and 10 μM in a concentration dependant manner (Fig. 5A). Hypoxia-mediated increases in vimentin mRNA levels were also attenuated by MRA2578 but only at 10 μM (Fig. 5B). As with siRNA-mediated silencing of P2Y6, there was no change in the mRNA levels of N-cadherin, Snail and Twist, or the CD44/CD24 ratio. Given the association between the mesenchymal phenotype and cancer cell migration (Sahlgren et al., 2008), the effects of MRS2578 on the cellular migration of mesenchymal-like MDA-MB-231 breast cancer cells was determined to evaluate the possible role of P2Y6 in the migration of mesenchymal breast cancer cells.

3.4. Pharmacological inhibition of P2Y6 reduces cellular migration of the mesenchymal like MDA-MB-231 cell line

The effect of P2Y6 pharmacological inhibition on cellular migration of MDA-MB-231 (a mesenchymal-like breast cancer cell line (Heiser et al., 2012)) was assessed using an Oris™ Cell Migration Assay. Pharmacological inhibition of P2Y6 with MRS2578 (1 μM and 10μM) significantly reduced cell migration of MDA-MB-231 cells (Fig.6).

3.5. Assessment of P2Y6 in breast cancer cell lines and tumor molecular subtypes, and its association with overall survival

The Basal breast cancer molecular subtype is often associated with high levels of EMT markers, an aggressive phenotype and poor clinical outcomes (Sarrio et al., 2008). In order to determine the potential clinical significance of P2Y6 in breast cancer, we investigated the gene expression profile of P2Y6 in human breast cancer cell lines as well as human breast tumors. Despite its up-regulation in both EGF and hypoxia-induced EMT, P2Y6 mRNA levels were not significantly higher in Basal B/ mesenchymal cell lines compared to other cell line subgroups (Fig. 7A). However, analysis of P2Y6 in gene expression data from breast tumors representing four transcriptional subtypes showed elevated P2Y6 levels in Basal breast cancer subtypes compared to Luminal A and Luminal B subtypes (Fig. 7B). To evaluate the association between the level of P2Y6 and breast cancer prognosis, overall survival analysis of 1115 patients using the Kaplan-Meier Plotter was assessed. Breast cancer patients with high P2Y6 levels showed significantly reduced overall survival rates compared to patients with low levels of P2Y6 (Fig. 7Ci).This reduction in overall survival does not appear to be solely due to the correlation between P2Y6 and the Basal subtype (which is associated with poor prognosis) since P2Y6 levels were also clearly associated with poorer prognosis in Luminal A breast cancers (Fig. 7Cii). This association was not observed in other subtypes (data not shown).

4. Discussion

Extracellular nucleotides are largely secreted in response to pathologic conditions such as ischemia, hypoxia, or acute inflammation (Lazarowski et al., 2003). The tumor microenvironment is therefore rich in ATP, where ATP acts as a signaling molecule and a pro-inflammatory mediator (Di Virgilio, 2012). Increased concentrations of extracellular ATP have been reported in the

tumorinterstitium compared to healthy tissues, with levels of ATP reaching more than 700 μM (Munaron and Fiorio, 2009). Here we show that hypoxia changes the $[Ca^{2+}]_{CYT}$ response of MDA-MB-468 breast cancer cells to ATP. Hypoxia resulted in MDA-MB-468 breast cancer cells becoming less sensitive to ATP (reflected in a rightward shift in the concentration response curve and a significant increase in the EC_{50}). Hypoxia also produced a significant attenuation in the maximum $[Ca^{2+}]_{CYT}$ response elicited by ATP. The nature of the ATP-mediated response was also remodeled through a faster return to basal $[Ca^{2+}]_{CYT}$ levels. This remodeling is identical to that associated with EGF-induced EMT in MDA-MB-468 breast cancer cells (Davis et al., 2011). Hence, attenuation of responses to ATP-mediated Ca^{2+} signaling may be a universal consequence of EMT in breast cancer cells. Reduction in the sensitivity of breast cancer cells to ATP-mediated Ca^{2+}signaling may reflect an ability of breast cancer cells to acquire more migratory characteristics and escape the primary tumor, without risking excessive responses to the elevated ATP levels in the tumor microenvironment. Further studies are required to determine if a reduction in the sensitivity to ATP-mediated Ca^{2+}signaling is also present in EMT in other cancers, such as those of the prostate in response to hypoxia (Jiang et al., 2007) and ovary in response to TGF-β (Kitagawa et al., 1996).

Following the observed change in the response of hypoxic cells to ATP, we assessed the mRNA levels of a panel of P2X and P2Y receptors and observed a change in levels of a suite of purinergic receptors. Changes observed included the down-regulation of P2X4, P2X5, P2X7, P2Y1, P2Y11 receptors and the up-regulation of the P2Y6 receptor. Although ATP sensitivity was reduced by both EGF and hypoxia, the changes in purinergic receptor mRNA levels were not identical, and P2Y6 was identified as the only purinergic receptor that was up-regulated in both hypoxia and EGF-induced EMT. The other receptor up-regulated by EGF in MDA-MB-468 breast cancer cells, P2X5, was actually down-regulated in hypoxia. The difference in the remodeling of purinergic receptors in the two models of EMT indicates that breast cancer cells may differentially exploit changes in the expression of purinergic receptors that differ in their ATP affinity (Davis et al., 2012) and/or other mechanisms (e.g. post- translational modification) (Gonnord et al., 2009; Roberts et al., 2007) to achieve reduced sensitivity to ATP.Hypoxia may also induce purinergic receptor remodeling in cells which represent the mesenchymal state. Tafani et al (Tafani et al., 2011) reported an increase in P2X7 levels with hypoxia in MDA-MB-231 cells, which is a mesenchymal-likehuman breast cancer cell

line with constitutive expression of vimentin protein (Mendez et al., 2010), as well as HeLa and MCF-7 cells.

The up-regulation of P2Y6 with both EGF and hypoxia induced EMT, suggests that P2Y6 may be important in bestowing mesenchymal properties on breast cancer cells. Increased expression of P2Y6 mRNA was seen in Basal breast cancers, which overlap significantly with mesenchymal markers (Neve et al., 2006; Sarrio et al., 2008). The association of P2Y6 with poor overall survival supports a role for P2Y6 in pathways important in breast cancer metastasis. High levels of P2Y6 in Luminal A breast cancers with poorer overall survival may indicate the presence of a subset of ER-positive tumors that express mesenchymal features including P2Y6. Overexpression of P2Y6 mRNA is a feature of human melanomas (White et al., 2005), human neuroblastoma cells (Lee et al., 2003), human prostate carcinoma cells (Janssens and Boeynaems, 2001), human colonic Caco-2 adenocarcinoma cells (McAlroy et al., 2000), A549 human lung cancer cells (Zhao et al., 2000) and human pancreatic cancer biopsies (Kunzli et al., 2007). Our studies now show that P2Y6 is also up-regulated in Basal breast cancers.

Silencing and pharmacological inhibition of P2Y6 resulted in reduction of hypoxia-induced vimentin expression, indicating the role of P2Y6 as a regulator of specific aspects of EMT in this model. The effects of siRNA silencing and pharmacological inhibition of P2Y6 were more pronounced on the expression of vimentin protein than mRNA, suggesting the mechanism of regulation is not entirely transcriptional. Indeed P2Y6 silencing and inhibition had no significant effect on the induction of the EMT-inducing transcription factors Twist and Snail, which are significantly increased as part of the EMT response to hypoxia. EMT is a complex molecular and cellular process whereby different EMT markers appear more pivotal in specific downstream pathways important in the acquisition of key mesenchymal phenotypes than others. For instance, Snail is a key regulator of E-cadherin expression (Cano et al., 2000), and Twist plays an important role in the inactivation of cellular senescence (Ansieau et al., 2008). Vimentin was the only assessed hypoxia-induced EMT marker in MDA-MB-468 breast cancer cells that was affected by P2Y6 silencing and pharmacological inhibition. Vimentin has a critical role in the changes in cell shape, adhesion and motility that occur as a consequence of EMT (Mendez et al., 2010). Indeed, we demonstrated that the pharmacological inhibition of P2Y6 resulted in a reduction in the cellular migration of mesenchymal like MDA-MB-231

breast cancer cells. In this context it is interesting to note that P2Y2 was recently shown to regulate the migration of human hepatocellular carcinoma cells (Xie et al., 2014), prostate cancer cells (Li et al., 2013) and MCF-7 breast cancer cells (Chadet et al., 2014). The role of P2Y6 in hypoxia-induced vimentin expression in MDA-MB-468 cells and in MDA-MB-231 cell migration, the elevation of P2Y6 in basal-like breast cancers and breast cancers with lower overall survival, collectively identify P2Y6 as a potential therapeutic target for breast cancer metastasis.

5. Conclusion

In summary, these studies demonstrate that hypoxia in MDA-MB-468 breast cancer cells is associated with alterations in ATP-mediated Ca^{2+}signaling. Reduced sensitivity to ATP-mediated Ca^{2+}signaling as a consequence of EMT in breast cancer cells may bestow advantages to breast cancer cells in escaping the primary tumor microenvironment. However, the mechanism by which this is achieved appears to be distinct between growth factor (e.g. EGF) and hypoxia induced EMT. The identification of elevated P2Y6 in both hypoxia and EGF-induced EMT as well as Basal breast cancers and other breast cancers with poor overall survival, suggest that P2Y6 may play a role in specific aspects of breast cancer metastasis, The ability of P2Y6 pharmacological inhibition to attenuate hypoxia-induced vimentin expression and reduce the migration of MDA-MB-231 basal-like breast cancer cells identifies P2Y6 as a potential novel target for breast cancer metastasis.

Conflict of interest:The authors declare no conflict of interest

Acknowledgments

The research was supported by the National Health and Medical Research Council (NHMRC; project grants 569645 and 1022263) and the Queensland Cancer Council (1042819). PK was supported by the American Cancer Society (RSG-TBE-123001). EWT was funded in part by the EM*Pathy* Breast Cancer Network of the National Breast Cancer Foundation (CG-10-04), Australia, and benefited from support by the Victorian Government's Operational Infrastructure Support Program to St. Vincent's Institute.

Figure legends

Fig. 1. Induction of EMT by hypoxia in MDA-MB-468 cells.(**A**)Hypoxia (24 h) induces significant increases in mRNA levels of EMT-associated genes vimentin, N-cadherin, Twist, Snail, Zeb1, and CD44/CD24 ratio; ***$p< 0.0001$, **$p< 0.001$, *$p< 0.01$ compared with normoxia (unpaired t-test). Data are mean (+ SD) from three independent experiments. (**B**) Representative immunoblot (left) and densitometry data of mean (+ SD) from three independent experiments (right) shows significant up-regulation of vimentin protein with hypoxia (48 h); ***$p< 0.001$ compared with normoxia (unpaired t-test).(**C**) Representative immunoblot (left) and densitometry data of mean (+ SD) from three independent experiments (right) shows significant down-regulation of E-cadherin protein with hypoxia (48 h); ***$p< 0.001$ compared with normoxia (unpaired t-test).(**D**) Cells acquire spindle-shaped mesenchymal morphology after 48 h hypoxia. Scale bar: 50 µm.

Fig. 2. ATP-mediated Ca^{2+}signaling in MDA-MB-468 cells following hypoxia.(**A**) Average $[Ca^{2+}]_{CYT}$transients for hypoxic and normoxic cells stimulated with 1 mM ATP. (**B**) Assessment of$[Ca^{2+}]_{CYT}$in MDA-MB-468 cells incubated in hypoxic conditions for 24 h following stimulation with different concentrations of ATP. Graphs represent the mean (± SD) of relative peak $[Ca^{2+}]_{CYT}$ (inset - average EC_{50}; *$p< 0.05$ (unpaired t-test). (**C**) Mean percent $[Ca^{2+}]_{CYT}$recovery (+ SD) at 800 s with 10 µM, 100 µM and 1 mM of ATP. **$p< 0.01$ (unpaired t-test).

Fig. 3. Transcriptional profile of purinergic receptors is altered by hypoxia in MDA-MB-468 breast cancer cells.(**A**) Relative mRNA (as $-\Delta C_T$) of seven P2X and eight P2Y isoforms in normoxic (black) and hypoxic (red) conditions (■ denotes a target below the limit of detection ($C_T > 35$) in one or more replicates of hypoxic and normoxic samples; • denotes a target below the limit of detection ($C_T > 35$) in one or more replicates of hypoxic samples only). Bar represents the mean of triplicates. (**B**) Hypoxia induces a significant increase in P2Y6 receptor mRNA (24 h hypoxia) and (**C**) protein (48 h hypoxia) levels, mean (+ SD) of three independent experiments. *$P< 0.001$ (unpaired t-test). (**D**) Comparison of purinergic receptor mRNA changes associated with EGF and hypoxia models of EMT in MDA-MB-468 cellsshows that P2X4, P2X5, P2X7, P2Y1 and P2Y11 are down-regulated in hypoxia-induced EMT, and P2Y13 is down-regulated in EGF-induced EMT (left panel). P2Y6 is up-regulated by both EGF and hypoxia and P2X5 is up-regulated only with EGF (right panel). (**E**) siRNA-mediated silencing of HIF1α (shown as percent mRNA remaining relative to NT in the left panel),

attenuates hypoxia-induced P2Y6 mRNA up-regulation (right panel). *p< 0.05 (one-way ANOVA Benferroni multiple comparisons test), **p< 0.01 (unpaired t-test).

Fig. 4. Effect ofP2Y6 silencing on the expression of EMT markers induced by hypoxia. (**A**) siRNA mediated P2Y6 silencing shown as percent mRNA remaining relative to NT siRNA. (**B**) Representative immunoblot (left) and densitometry data of mean (+ SD) from three independent experiments (right) showsattenuation of 48 h hypoxia induced-vimentin protein expression by P2Y6 silencing. *p< 0.0001 compared with hypoxia NT (Benferroni one-way ANOVA). (C) P2Y6 silencing has no significant effect on the mRNA levels of vimentin, N-cadherin, Snail, Twist and CD44/CD24 ratio induced by hypoxia.NS = not significant (p> 0.05)

Fig. 5. Effect of P2Y6 pharmacological inhibition on the expression of EMT markers induced by hypoxia. (**A**)Representative immunoblot (left) and densitometry data of mean (+ SD) from three independent experiments (right)shows down-regulation of 24 h hypoxia-induced vimentin protein expression at 3 μM and 10 μM by the P2Y6 inhibitor, MRS2578. *p< 0.001 and **p< 0.0001 compared with hypoxia NT (Benferroni one-way ANOVA). (**B**) MRS2578 at 10 μM significantly reduced vimentin mRNA levels, however it had no significant effect on other EMT markers. *p< 0.001 compared with hypoxia NT (one-way ANOVA Benferroni multiple comparisons test)

Fig. 6. Effect of P2Y6 pharmacological inhibition on the migration of MDA-MB-231 cells. (**A**) Representative fluorescence images of (i) reference (where stoppers were removed immediately prior to imaging to show the original detection zone); and migration after 24 h with media containing (ii) DMSO (control) or (iii and iv) the P2Y6 inhibitor MRS2578 (1 μM and 10μM). (**B**). Cell migration was quantified as the percentage of migrated cell area normalized to the DMSO controls. Data are mean (+ SD) from three independent experiments performed in duplicate wells. *P< 0.05 (Benferroni one-way ANOVA).

Fig. 7. Expression of P2Y6 in breast cancer cell lines and tumor samples, and its association with patient survival. (**A**) Gene expression profiling of 49 breast cancer cell lines and 5 nonmalignant immortalized human mammary epithelial cells comprising three subgroups of Luminal, Basal A and Basal B/Mesenchymal . (**B**) Gene expression profile of 458 breast tumors revealed elevation of P2Y6

in Basal tumor subtypes. *** $p< 001$, Kruskall-Wallis test. (**C**) The Kaplan–Meier plot suggests that breast cancer patients with elevated levels of P2Y6 (n=651) show reduced overall survival rate compared to the remaining patients (n= 464), $P = 0.019$ (Ci). Luminal A breast cancers were the only subtype where high levels of P2Y6 were associated with reduced overall, $P = 0.03$ (Cii).

References

Akl, H., Bultynck, G., 2013. Altered Ca2+ signaling in cancer cells: Proto-oncogenes and tumor suppressors targeting IP3 receptors. Bba-Rev Cancer 1835, 180-193.

Ansieau, S., Bastid, J., Doreau, A., Morel, A.P., Bouchet, B.P., Thomas, C., Fauvet, F., Puisieux, I., Doglioni, C., Piccinin, S., Maestro, R., Voeltzel, T., Selmi, A., Valsesia-Wittmann, S., de Fromentel, C.C., Puisieux, A., 2008. Induction of EMT by twist proteins as a collateral effect of tumor-promoting inactivation of premature senescence. Cancer Cell 14, 79-89.

Balko, J.M., Schwarz, L.J., Bhola, N.E., Kurupi, R., Owens, P., Miller, T.W., Gomez, H., Cook, R.S., Arteaga, C.L., 2013. Activation of MAPK Pathways due to DUSP4 Loss Promotes Cancer Stem Cell-like Phenotypes in Basal-like Breast Cancer. Cancer Res. 73, 6346-6358.

Burnstock, G., Di, V.F., 2013. Purinergic signalling and cancer. Purinerg Signal. 9, 491-540.

Cannito, S., Novo, E., Compagnone, A., Valfre, d.B.L., Busletta, C., Zamara, E., Paternostro, C., Povero, D., Bandino, A., Bozzo, F., Cravanzola, C., Bravoco, V., Colombatto, S., Parola, M., 2008. Redox mechanisms switch on hypoxia-dependent epithelial-mesenchymal transition in cancer cells. Carcinogenesis 29, 2267-2278.

Cano, A., Perez-Moreno, M.A., Rodrigo, I., Locascio, A., Blanco, M.J., del Barrio, M.G., Portillo, F., Nieto, M.A., 2000. The transcription factor Snail controls epithelial-mesenchymal transitions by repressing E-cadherin expression. Nat. Cell Biol. 2, 76-83.

Chadet, S., Jelassi, B., Wannous, R., Angoulvant, D., Chevalier, S., Besson, P., Roger, S., 2014. The activation of P2Y2 receptors increases MCF-7 breast cancer cells migration through the MEK-ERK1/2 signalling pathway. Carcinogenesis 35, 1238-1247.

Chen, Y.F., Chiu, W.T., Chen, Y.T., Lin, P.Y., Huang, H.J., Chou, C.Y., Chang, H.C., Tang, M.J., Shen, M.R., 2011. Calcium store sensor stromal-interaction molecule 1-dependent signaling plays an important role in cervical cancer growth, migration, and angiogenesis. Proc. Natl. Acad. Sci. U. S. A. 108, 15225-15230.

Coakley, R.D., Sun, H., Clunes, L.A., Rasmussen, J.E., Stackhouse, J.R., Okada, S.F., Fricks, I., Young, S.L., Tarran, R., 2008. 17 beta-Estradiol inhibits Ca(2+)-dependent homeostasis of airway surface liquid volume in human cystic fibrosis airway epithelia. J. Clin. Investig. 118, 4025-4035.

Cooke, V.G., LeBleu, V.S., Keskin, D., Khan, Z., O'Conne, J.T., Teng, Y., Duncan, M.B., Xie, L., Maeda, G., Vong, S., Sugimoto, H., Rocha, R.M., Damascena, A., Brentani, R.R., Kalluri, R., 2012. Pericyte Depletion Results in Hypoxia-Associated Epithelial-to-Mesenchymal Transition and Metastasis Mediated by Met Signaling Pathway. Cancer Cell 21, 66-81.

Cursons, J., Leuchowius, K.J., Waltham, M., Tomaskovic-Crook, E., Foroutan, M., Bracken, C.P., Redfern, A., Crampin, E.J., Street, I., Davis, M.J., Thompson, E.W., 2015. Stimulus-dependent differences in signalling regulate epithelial-mesenchymal plasticity and change the effects of drugs in breast cancer cell lines. Cell communication and signaling : CCS 13, 26.

Davis, F.M., Azimi, I., Faville, R.A., Peters, A.A., Jalink, K., Putney, J.W., Jr., Goodhill, G.J., Thompson, E.W., Roberts-Thomson, S.J., Monteith, G.R., 2013. Induction of epithelial-mesenchymal transition (EMT) in breast cancer cells is calcium signal dependent. Oncogene 33, 2307-16.

Davis, F.M., Kenny, P.A., Soo, E.T., van Denderen, B.J., Thompson, E.W., Cabot, P.J., Parat, M.O., Roberts-Thomson, S.J., Monteith, G.R., 2011. Remodeling of purinergic receptor-mediated Ca2+ signaling as a consequence of EGF-induced epithelial-mesenchymal transition in breast cancer cells. PLoS ONE 6, e23464.

Davis, F.M., Peters, A.A., Grice, D.M., Cabot, P.J., Parat, M.O., Roberts-Thomson, S.J., Monteith, G.R., 2012. Non-stimulated, agonist-stimulated and store-operated Ca2+ influx in MDA-MB-468 breast cancer cells and the effect of EGF-induced EMT on calcium entry. PLoS ONE 7, e36923.

Di Virgilio, F., 2012. Purines, purinergic receptors, and cancer. Cancer Res. 72, 5441-5447.

Giricz, O., Calvo, V., Peterson, E.A., Abouzeid, C.M., Kenny, P.A., 2013. TACE-dependent TGFalpha shedding drives triple-negative breast cancer cell invasion. Int. J. Cancer 133, 2587-2595.

Gonnord, P., Delarasse, C., Auger, R., Benihoud, K., Prigent, M., Cuif, M.H., Lamaze, C., Kanellopoulos, J.M., 2009. Palmitoylation of the P2X7 receptor, an ATP-gated channel, controls its expression and association with lipid rafts. FASEB journal : official publication of the Federation of American Societies for Experimental Biology 23, 795-805.

Grice, D.M., Vetter, I., Faddy, H.M., Kenny, P.A., Roberts-Thomson, S.J., Monteith, G.R., 2010. Golgi calcium pump secretory pathway calcium ATPase 1 (SPCA1) is a key regulator of insulin-like growth factor receptor (IGF1R) processing in the basal-like breast cancer cell line MDA-MB-231. J. Biol. Chem. 285, 37458-37466.

Griffiths, G., Lucocq, J.M., 2014. Antibodies for immunolabeling by light and electron microscopy: not for the faint hearted. Histochem. Cell Biol. 142, 347-360.

Grunert, S., Jechlinger, M., Beug, H., 2003. Diverse cellular and molecular mechanisms contribute to epithelial plasticity and metastasis. Nat. Rev. Mol. Cell Biol. 4, 657-665.

Gyorffy, B., Lanczky, A., Eklund, A.C., Denkert, C., Budczies, J., Li, Q.Y., Szallasi, Z., 2010. An online survival analysis tool to rapidly assess the effect of 22,277 genes on breast cancer prognosis using microarray data of 1,809 patients. Breast Cancer Res. Treat. 123, 725-731.

Heiser, L.M., Sadanandam, A., Kuo, W.L., Benz, S.C., Goldstein, T.C., Ng, S., Gibb, W.J., Wang, N.J., Ziyad, S., Tong, F., Bayani, N., Hu, Z., Billig, J.I., Dueregger, A., Lewis, S., Jakkula, L., Korkola, J.E., Durinck, S., Pepin, F., Guan, Y., Purdom, E., Neuvial, P., Bengtsson, H., Wood, K.W., Smith, P.G., Vassilev, L.T., Hennessy, B.T., Greshock, J., Bachman, K.E., Hardwicke, M.A., Park, J.W., Marton, L.J., Wolf, D.M., Collisson, E.A., Neve, R.M., Mills, G.B., Speed, T.P., Feiler, H.S., Wooster, R.F., Haussler, D., Stuart, J.M., Gray, J.W., Spellman, P.T., 2012. Subtype and pathway specific responses to anticancer compounds in breast cancer. Proc. Natl. Acad. Sci. U. S. A. 109, 2724-2729.

Janssens, R., Boeynaems, J.M., 2001. Effects of extracellular nucleotides and nucleosides on prostate carcinoma cells. Br. J. Pharmacol. 132, 536-546.

Jiang, J., Tang, Y.L., Liang, X.H., 2011. EMT: a new vision of hypoxia promoting cancer progression. Cancer Biol. Ther. 11, 714-723.

Jiang, Y.G., Luo, Y., He, D.L., Li, X., Zhang, L.L., Peng, T., Li, M.C., Lin, Y.H., 2007. Role of Wnt/beta-catenin signaling pathway in epithelial-mesenchymal transition of human prostate cancer induced by hypoxia-inducible factor-1alpha. Int. J. Urol. 14, 1034-1039.

Jo, M., Lester, R.D., Montel, V., Eastman, B., Takimoto, S., Gonias, S.L., 2009. Reversibility of epithelial-mesenchymal transition (EMT) induced in breast cancer cells by activation of urokinase receptor-dependent cell signaling. J. Biol. Chem. 284, 22825-22833.

Kitagawa, K., Murata, A., Matsuura, N., Tohya, K., Takaichi, S., Monden, M., Inoue, M., 1996. Epithelial-mesenchymal transformation of a newly established cell line from ovarian adenosarcoma by transforming growth factor-beta1. International journal of cancer. Int. J. Cancer 66, 91-97.

Koboldt, D.C., Fulton, R.S., McLellan, M.D., Schmidt, H., Kalicki-Veizer, J., McMichael, J.F., Fulton, L.L., Dooling, D.J., Ding, L., Mardis, E.R., Wilson, R.K., Ally, A., Balasundaram, M., Butterfield, Y.S.N., Carlsen, R., Carter, C., Chu, A., Chuah, E., Chun, H.J.E., Coope, R.J.N., Dhalla, N., Guin, R., Hirst, C., Hirst, M., Holt, R.A., Lee, D., Li, H.Y.I., Mayo, M., Moore, R.A., Mungall, A.J., Pleasance, E., Robertson, A.G., Schein, J.E., Shafiei, A., Sipahimalani, P., Slobodan, J.R., Stoll, D., Tam, A., Thiessen, N., Varhol, R.J., Wye, N., Zeng, T., Zhao, Y.J., Birol, I., Jones, S.J.M., Marra, M.A., Cherniack, A.D., Saksena, G., Onofrio, R.C., Pho, N.H., Carter, S.L., Schumacher, S.E., Tabak, B., Hernandez, B., Gentry, J., Nguyen, H., Crenshaw, A., Ardlie, K., Beroukhim, R., Winckler, W., Getz, G., Gabriel, S.B., Meyerson, M., Chin, L., Park, P.J., Kucherlapati, R., Hoadley, K.A., Auman, J.T., Fan, C., Turman, Y.J., Shi, Y., Li, L., Topal, M.D., He, X.P., Chao, H.H., Prat, A., Silva, G.O., Iglesia, M.D., Zhao, W., Usary, J., Berg, J.S., Adams, M., Booker, J., Wu, J.Y., Gulabani, A., Bodenheimer, T., Hoyle, A.P., Simons, J.V., Soloway, M.G., Mose, L.E., Jefferys, S.R., Balu, S., Parker, J.S., Hayes, D.N., Perou, C.M., Malik, S., Mahurkar, S., Shen, H., Weisenberger, D.J., Triche, T., Lai, P.H., Bootwalla, M.S., Maglinte, D.T., Berman, B.P., Van den Berg, D.J., Baylin, S.B., Laird, P.W., Creighton, C.J., Donehower, L.A., Getz, G., Noble, M., Voet, D., Saksena, G., Gehlenborg, N., DiCara, D., Zhang, J.H., Zhang, H.L., Wu, C.J., Liu, S.Y., Lawrence, M.S., Zou, L.H., Sivachenko, A., Lin, P., Stojanov, P., Jing, R., Cho, J., Sinha, R., Park, R.W., Nazaire, M.D., Robinson, J., Thorvaldsdottir, H., Mesirov, J., Park, P.J., Chin, L., Reynolds, S., Kreisberg, R.B., Bernard, B., Bressler, R., Erkkila, T., Lin, J., Thorsson, V., Zhang, W., Shmulevich, I., Ciriello, G., Weinhold, N., Schultz, N., Gao, J.J., Cerami, E., Gross, B., Jacobsen, A., Sinha, R., Aksoy, B.A., Antipin, Y., Reva, B., Shen, R.L., Taylor, B.S., Ladanyi, M., Sander, C., Anur, P., Spellman, P.T., Lu, Y.L., Liu, W.B., Verhaak, R.R.G., Mills, G.B., Akbani, R., Zhang, N.X., Broom, B.M., Casasent, T.D., Wakefield, C., Unruh, A.K., Baggerly, K., Coombes, K., Weinstein, J.N., Haussler, D., Benz, C.C., Stuart, J.M., Benz, S.C., Zhu, J.C., Szeto, C.C., Scott, G.K., Yau, C., Paul, E.O., Carlin, D., Wong, C., Sokolov, A., Thusberg, J., Mooney, S., Ng, S., Goldstein, T.C., Ellrott, K., Grifford, M., Wilks, C., Ma, S., Craft, B., Yan, C.H., Hu, Y., Meerzaman, D., Gastier-Foster, J.M., Bowen, J., Ramirez, N.C., Black, A.D., Pyatt, R.E., White, P., Zmuda, E.J., Frick, J., Lichtenberg, T., Brookens, R., George, M.M., Gerken, M.A., Harper, H.A., Leraas, K.M., Wise, L.J., Tabler, T.R., McAllister, C., Barr, T., Hart-Kothari, M., Tarvin, K., Saller, C., Sandusky, G., Mitchell, C., Iacocca, M.V., Brown, J., Rabeno, B., Czerwinski, C., Petrelli, N., Dolzhansky, O., Abramov, M., Voronina, O., Potapova, O., Marks, J.R., Suchorska, W.M., Murawa, D., Kycler, W., Ibbs, M., Korski, K., Spychala, A., Murawa, P., Brzezinski, J.J., Perz, H., Lazniak, R., Teresiak, M., Tatka, H., Leporowska, E., Bogusz-Czerniewicz, M., Malicki, J., Mackiewicz, A., Wiznerowicz, M., Le, X.V., Kohl, B., Tien, N.V., Thorp, R., Bang, N.V., Sussman, H., Phu, B.D., Hajek, R., Hung, N.P., Tran, V.T.P., Thang, H.Q., Khan, K.Z., Penny, R., Mallery, D., Curley, E., Shelton, C., Yena, P., Ingle, J.N., Couch, F.J., Lingle, W.L., King, T.A., Gonzalez-Angulo, A.M., Mills, G.B., Dyer, M.D., Liu, S.Y., Meng, X.L., Patangan, M., Waldman, F., Stoppler, H., Rathmell, W.K., Thorne, L., Huang, M., Boice, L., Hill, A., Morrison, C., Gaudioso, C., Bshara, W., Daily, K., Egea, S.C., Pegram, M.D., Gomez-Fernandez, C., Dhir, R., Bhargava, R., Brufsky, A., Shriver, C.D., Hooke, J.A., Campbell, J.L., Mural, R.J., Hu, H., Somiari, S., Larson, C., Deyarmin, B., Kvecher, L., Kovatich, A.J., Ellis, M.J., King, T.A., Hu, H., Couch, F.J., Mural, R.J., Stricker, T., White, K., Olopade, O., Ingle, J.N., Luo, C.Q., Chen, Y.Q., Marks, J.R., Waldman, F., Wiznerowicz, M., Bose, R., Chang, L.W., Beck, A.H., Gonzalez-Angulo, A.M., Pihl, T., Jensen, M., Sfeir, R., Kahn, A., Chu, A., Kothiyal, P., Wang, Z.N., Snyder, E., Pontius, J., Ayala, B., Backus, M., Walton, J., Baboud, J., Berton, D., Nicholls, M., Srinivasan, D., Raman, R., Girshik, S., Kigonya, P., Alonso, S., Sanbhadti, R., Barletta, S., Pot, D., Sheth, M., Demchok, J.A., Shaw, K.R.M., Yang, L.M., Eley, G., Ferguson, M.L., Tarnuzzer, R.W., Zhang, J.S., Dillon, L.A.L., Buetow, K., Fielding, P., Ozenberger, B.A., Guyer, M.S., Sofia, H.J., Palchik, J.D., Network, C.G.A., 2012. Comprehensive molecular portraits of human breast tumours. Nature 490, 61-70.

Kunzli, B.M., Berberat, P.O., Giese, T., Csizmadia, E., Kaczmarek, E., Baker, C., Halaceli, I., Buchler, M.W., Friess, H., Robson, S.C., 2007. Upregulation of CD39/NTPDases and P2 receptors in human pancreatic disease. Am. J. Physiol. Gastrointest. Liver Physiol 292, G223-G230.

Lazarowski, E.R., Boucher, R.C., Harden, T.K., 2003. Mechanisms of release of nucleotides and integration of their action as P2X- and P2Y-receptor activating molecules. Mol. Pharmacol. 64, 785-795.

Lee, H., Choi, B.H., Suh, B.C., Lee, S.K., Kim, K.T., 2003. Attenuation of signal flow from P2Y6 receptor by protein kinase C-alpha in SK-N-BE(2)C human neuroblastoma cells. J. Neurochem. 85, 1043-1053.

Li, W.H., Qiu, Y., Zhang, H.Q., Liu, Y., You, J.F., Tian, X.X., Fang, W.G., 2013. P2Y2 receptor promotes cell invasion and metastasis in prostate cancer cells. Br. J. Cancer 109, 1666-1675.

Lundgren, K., Nordenskjold, B., Landberg, G., 2009. Hypoxia, Snail and incomplete epithelial-mesenchymal transition in breast cancer. Br. J. Cancer 101, 1769-1781.

Maehara, Y., Kusumoto, H., Anai, H., Kusumoto, T., Sugimachi, K., 1987. Human-Tumor Tissues Have Higher Atp Contents Than Normal-Tissues. Clin. Chim. Acta 169, 341-343.

Mamedova, L.K., Joshi, B.V., Gao, Z.G., von Kugelgen, I., Jacobson, K.A., 2004. Diisothiocyanate derivatives as potent, insurmountable antagonists of P2y(6) nucleotide receptors. Biochem. Pharmacol. 67, 1763-1770.

McAlroy, H.L., Ahmed, S., Day, S.M., Baines, D.L., Wong, H.Y., Yip, C.Y., Ko, W.H., Wilson, S.M., Collett, A., 2000. Multiple P2Y receptor subtypes in the apical membranes of polarized epithelial cells. Br. J. Pharmacol. 131, 1651-1658.

Mendez, M.G., Kojima, S.I., Goldman, R.D., 2010. Vimentin induces changes in cell shape, motility, and adhesion during the epithelial to mesenchymal transition. FASEB J. 24, 1838-1851.

Misra, A., Pandey, C., Sze, S.K., Thanabalu, T., 2012. Hypoxia activated EGFR signaling induces epithelial to mesenchymal transition (EMT). PLoS ONE 7, e49766.

Munaron, L., Fiorio, P.A., 2009. Endothelial calcium machinery and angiogenesis: understanding physiology to interfere with pathology. Curr. Med. Chem. 16, 4691-4703.

Neve, R.M., Chin, K., Fridlyand, J., Yeh, J., Baehner, F.L., Fevr, T., Clark, L., Bayani, N., Coppe, J.P., Tong, F., Speed, T., Spellman, P.T., DeVries, S., Lapuk, A., Wang, N.J., Kuo, W.L., Stilwell, J.L., Pinkel, D., Albertson, D.G., Waldman, F.M., McCormick, F., Dickson, R.B., Johnson, M.D., Lippman, M., Ethier, S., Gazdar, A., Gray, J.W., 2006. A collection of breast cancer cell lines for the study of functionally distinct cancer subtypes. Cancer Cell 10, 515-527.

Pellegatti, P., Raffaghello, L., Bianchi, G., Piccardi, F., Pistoia, V., Di Virgilio, F., 2008. Increased Level of Extracellular ATP at Tumor Sites: In Vivo Imaging with Plasma Membrane Luciferase. PLoS ONE 3 e2599.

Polyak, K., Weinberg, R.A., 2009. Transitions between epithelial and mesenchymal states: acquisition of malignant and stem cell traits. Nat. Rev. Cancer 9, 265-273.

Prat, A., Parker, J.S., Karginova, O., Fan, C., Livasy, C., Herschkowitz, J.I., He, X., Perou, C.M., 2010. Phenotypic and molecular characterization of the claudin-low intrinsic subtype of breast cancer. Breast cancer research 12, R68.

Prevarskaya, N., Skryma, R., Shuba, Y., 2011. Calcium in tumour metastasis: new roles for known actors. Nat. Rev. Cancer 11, 609-618.

Roberts, V.H., Webster, R.P., Brockman, D.E., Pitzer, B.A., Myatt, L., 2007. Post-Translational Modifications of the P2X(4) purinergic receptor subtype in the human placenta are altered in preeclampsia. Placenta 28, 270-277.

Roderick, H.L., Cook, S.J., 2008. Ca2+ signalling checkpoints in cancer: remodelling Ca2+ for cancer cell proliferation and survival. Nat. Rev. Cancer 8, 361-375.

Ruan, K., Song, G., Ouyang, G., 2009. Role of hypoxia in the hallmarks of human cancer. J. Cell. Biochem. 107, 1053-1062.

Sahlgren, C., Gustafsson, M.V., Jin, S., Poellinger, L., Lendahl, U., 2008. Notch signaling mediates hypoxia-induced tumor cell migration and invasion. Proc. Natl. Acad. Sci. U. S. A. 105, 6392-6397.

Salnikov, A.V., Liu, L., Platen, M., Gladkich, J., Salnikova, O., Ryschich, E., Mattern, J., Moldenhauer, G., Werner, J., Schemmer, P., Buchler, M.W., Herr, I., 2012. Hypoxia induces EMT in low and highly aggressive pancreatic tumor cells but only cells with cancer stem cell characteristics acquire pronounced migratory potential. PLoS ONE 7, e46391.

Sarrio, D., Rodriguez-Pinilla, S.M., Hardisson, D., Cano, A., Moreno-Bueno, G., Palacios, J., 2008. Epithelial-mesenchymal transition in breast cancer relates to the basal-like phenotype. Cancer Res. 68, 989-997.

Shaikh, D., Zhou, Q., Chen, T., Ibe, J.C., Raj, J.U., Zhou, G., 2012. cAMP-dependent protein kinase is essential for hypoxia-mediated epithelial-mesenchymal transition, migration, and invasion in lung cancer cells. Cell. Signal. 24, 2396-2406.

Tafani, M., Schito, L., Pellegrini, L., Villanova, L., Marfe, G., Anwar, T., Rosa, R., Indelicato, M., Fini, M., Pucci, B., Russo, M.A., 2011. Hypoxia-increased RAGE and P2X7R expression regulates tumor cell invasion through phosphorylation of Erk1/2 and Akt and nuclear translocation of NF-kappa B. Carcinogenesis 32, 1167-1175.

Thiery, J.P., 2002. Epithelial-mesenchymal transitions in tumour progression. Nat. Rev. Cancer 2, 442-454.

Thiery, J.P., Sleeman, J.P., 2006. Complex networks orchestrate epithelial-mesenchymal transitions. Nat. Rev. Mol. Cell Biol. 7, 131-142.

White, N., Ryten, M., Clayton, E., Butler, P., Burnstock, G., 2005. P2Y purinergic receptors regulate the growth of human melanomas. Cancer Lett. 224, 81-91.

Xie, R., Xu, J., Wen, G., Jin, H., Liu, X., Yang, Y., Ji, B., Jiang, Y., Song, P., Dong, H., Tuo, B., 2014. The P2Y2 Nucleotide Receptor Mediates the Proliferation and Migration of Human Hepatocellular Carcinoma Cells Induced by ATP. J. Biol.Chem 289, 19137-19149.

Yu, W.Q., Hill, W.G., 2013. Lack of specificity shown by P2Y(6) receptor antibodies. N-S Arch Pharmacol 386, 885-891.

Zhang, L., Huang, G., Li, X., Zhang, Y., Jiang, Y., Shen, J., Liu, J., Wang, Q., Zhu, J., Feng, X., Dong, J., Qian, C., 2013. Hypoxia induces epithelial-mesenchymal transition via activation of SNAI1 by hypoxia-inducible factor -1alpha in hepatocellular carcinoma. BMC Cancer 13, 108.

Zhao, D.M., Xue, H.H., Chida, K., Suda, T., Oki, W., Kanai, M., Uchida, C., Ichiyama, A., Nakamura, H., 2000. Effect of erythromycin on ATP-induced intracellular calcium response in A549 cells. Am J Physiol-Lung C 278, L726-L736.

Figure 1
Click here to download high resolution image

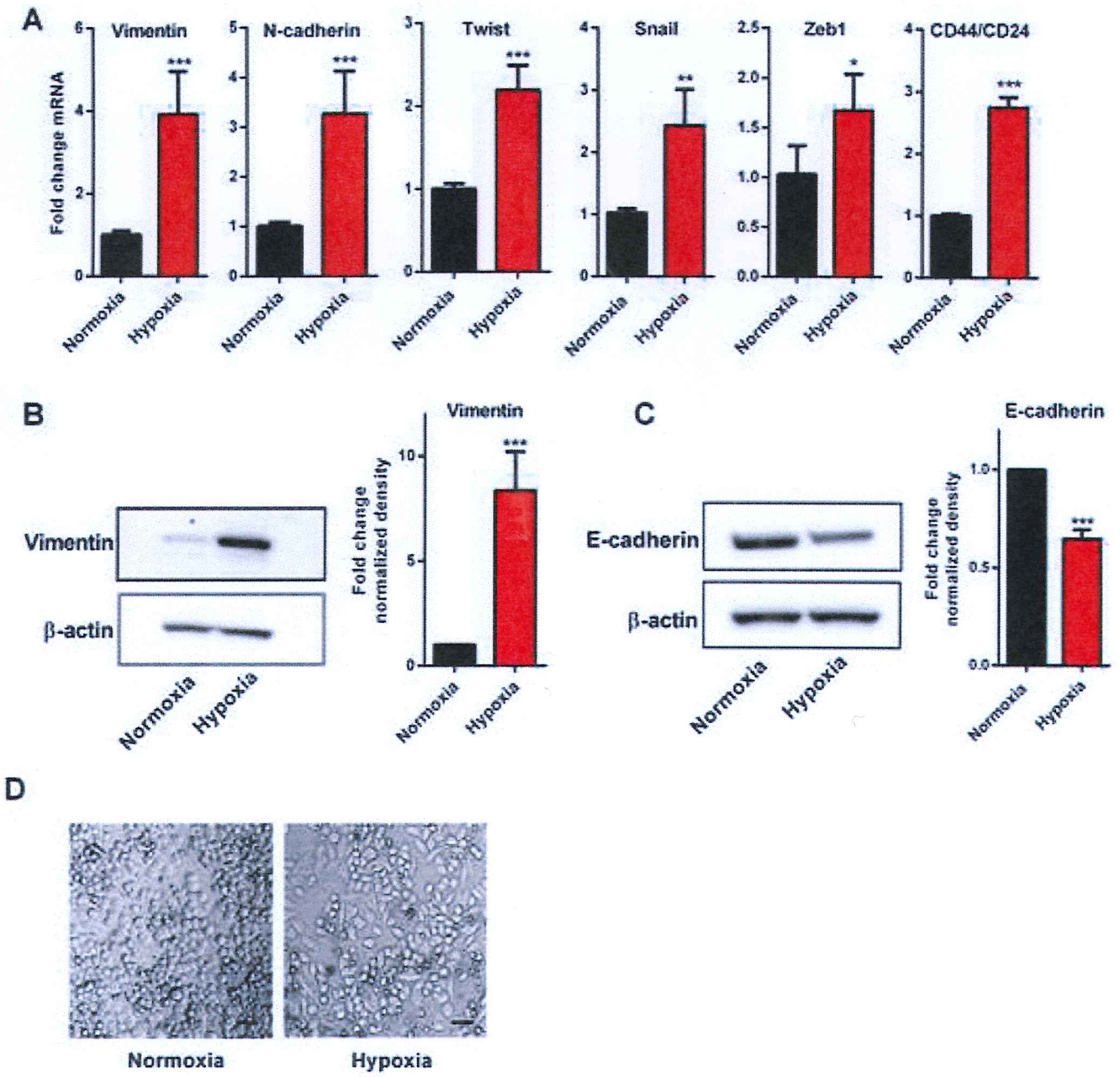

Figure 2
Click here to download high resolution image

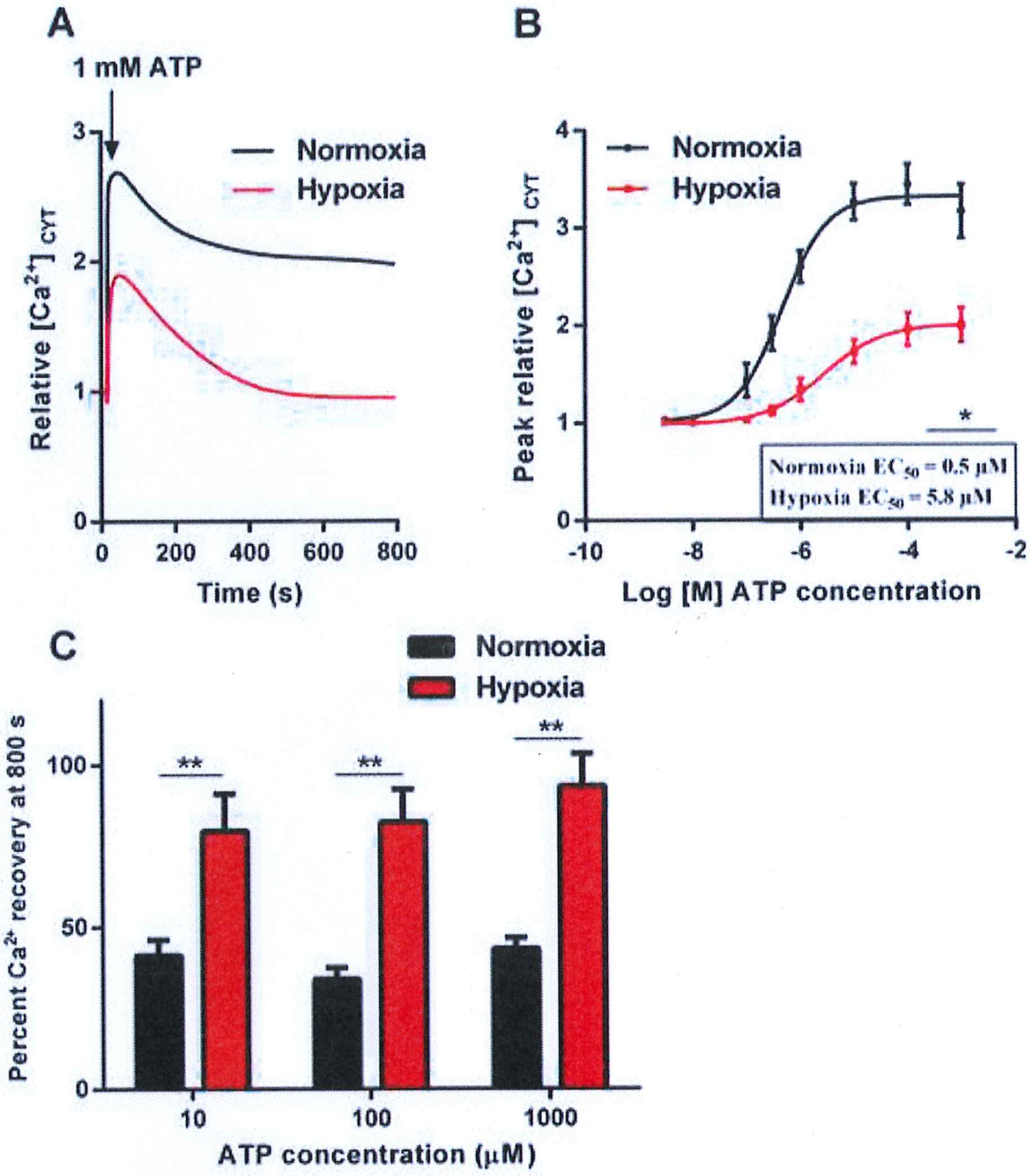

Figure 3
Click here to download high resolution image

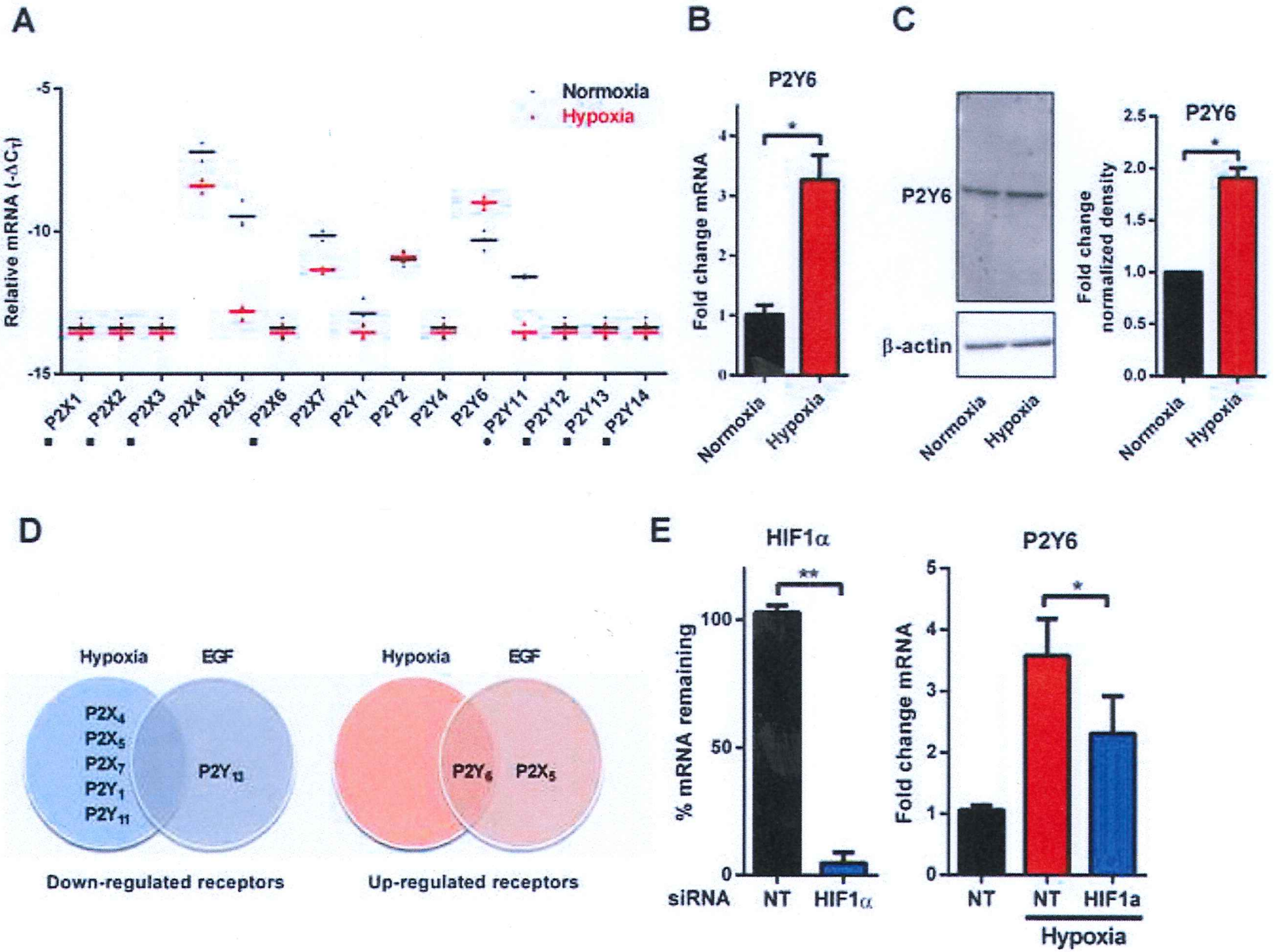

Figure 4
Click here to download high resolution image

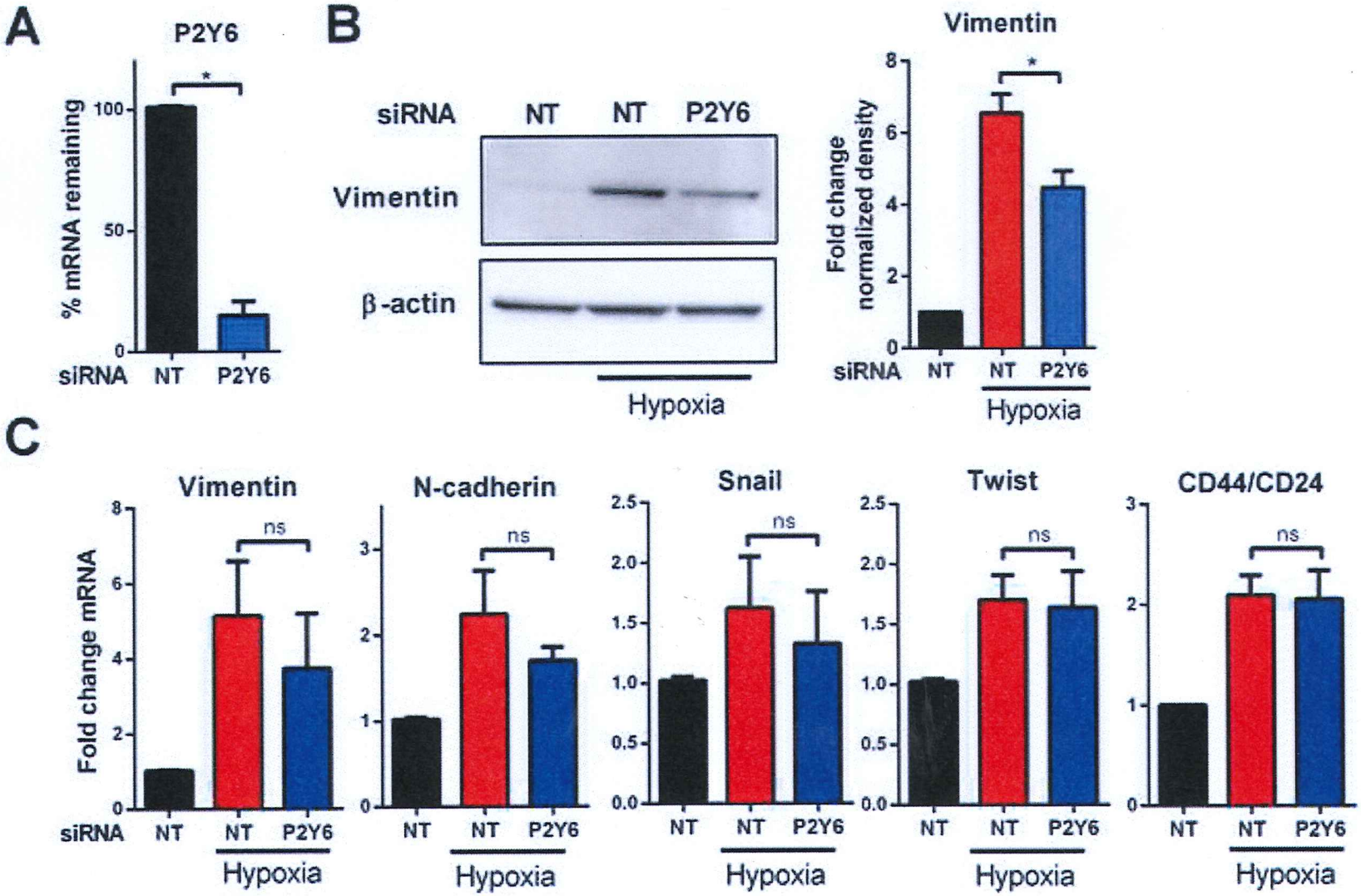

Figure 5
Click here to download high resolution image

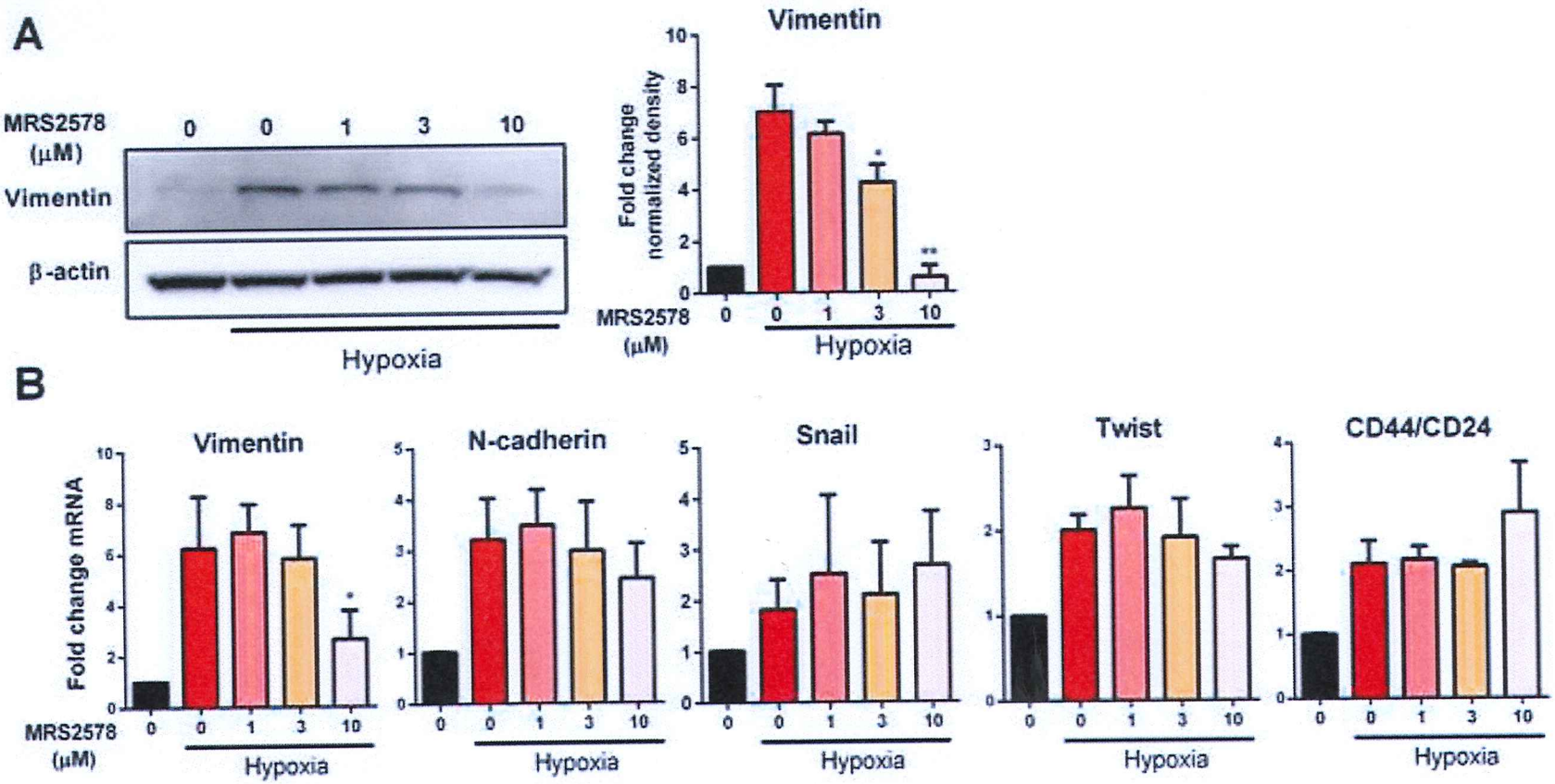

Figure 6
Click here to download high resolution image

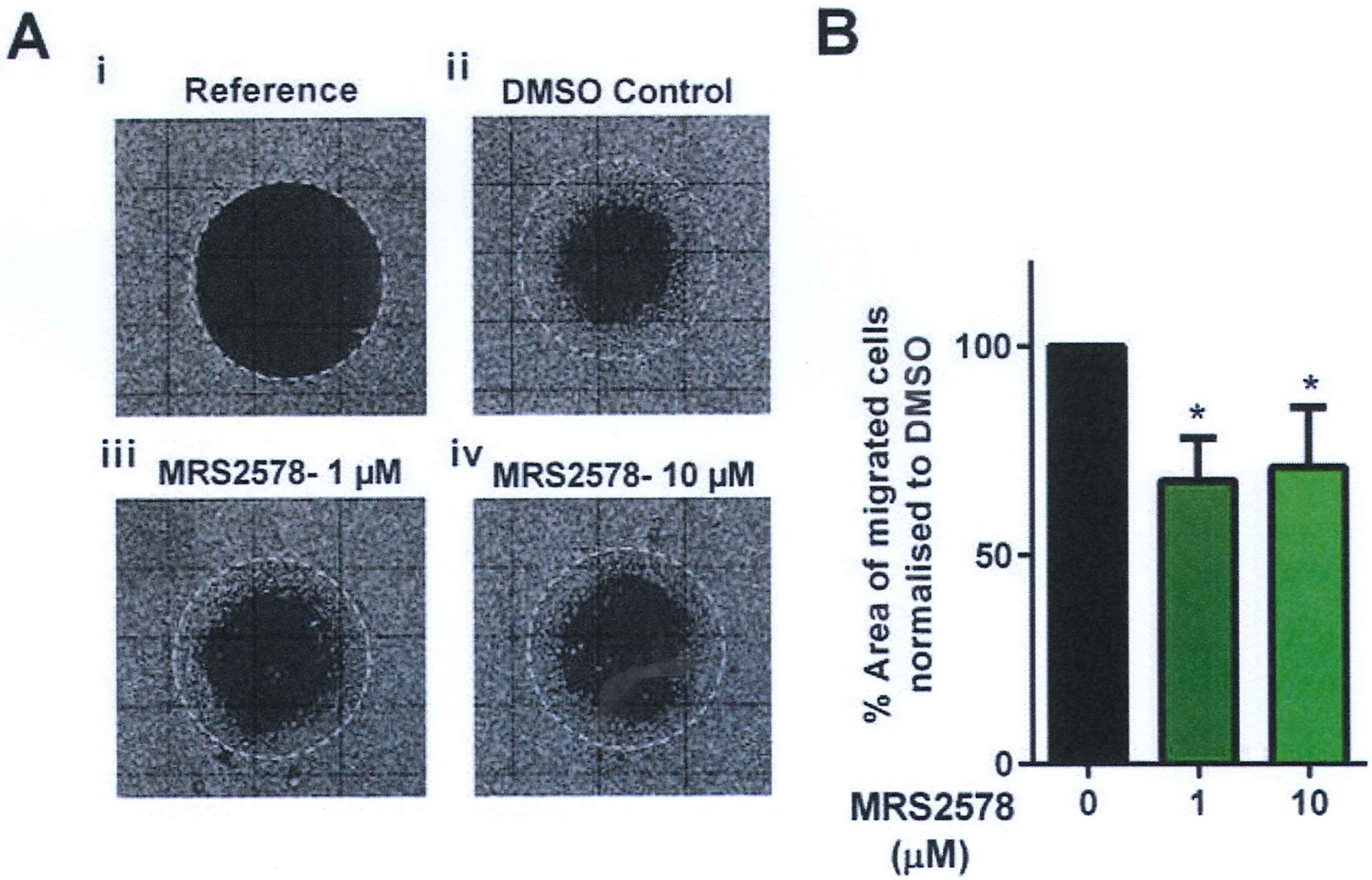

Figure 7
Click here to download high resolution image

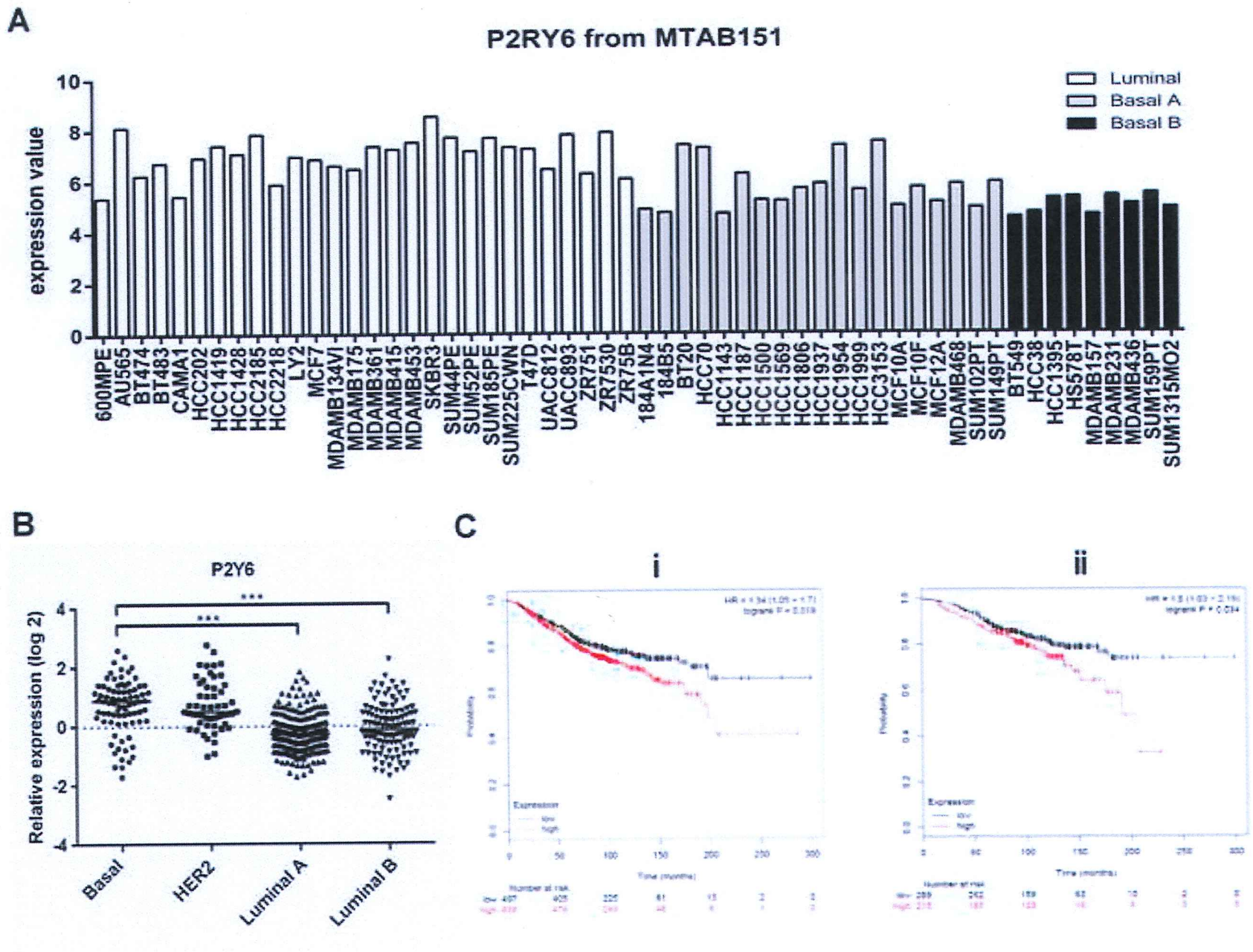

Supplementary material for online publication only

Click here to download Supplementary material for online publication only: Supplementary Table S1.docx